

Full-Section Support Technology for Mining Roadways in "Three-Soft" Unstable Thick Coal Seams

ZongMin Song

School of Energy Science and Engineering, Henan Polytechnic University, Jiaozuo, Henan 454000, China
Email: szm001104@163.com

How to cite this paper: Song, Z. M. (2026). Full-section support technology for mining roadways in "three-soft" unstable thick coal seams. *Academic Journal of Emerging Technologies*, 3(1), 120–134. ISSN Print: 3104-4417, ISSN Online: 3104-4425. <https://doi.org/10.63313/AJET.9060>
Published: 2026-05-22

Copyright © 2026 by author(s) and Erytis Publishing Limited.
This work is licensed under the Creative Commons Attribution International License (CC BY 4.0).
<http://creativecommons.org/licenses/by/4.0/>



Abstract

The main coal seam of Xingcun Coal Mine is a typical "three-soft" unstable coal seam, where mining roadways suffer from severe deformation and cannot remain stable despite repeated repairs and expansions during service. In this study, borehole inspection was employed to detect the development of fractures in the surrounding rock of the mining roadway, and numerical simulation was conducted to compare and analyze the plastic zone distribution and displacement characteristics of the roadway surrounding rock under four support schemes: U-shaped steel support alone; U-shaped steel support combined with roof and sidewall anchor cables; U-shaped steel support combined with full-section anchor cables; and U-shaped steel support combined with full-section anchor cables and grouting. The differences among these support schemes in controlling surrounding rock stability were elucidated. On this basis, a combined support scheme of "U-shaped steel support + full-section anchor cables + grouting" was proposed. The results indicate that the deformation of the roadway surrounding rock and the floor heave were significantly reduced, and the roadway maintained a favorable profile. During the observation period, the convergence between the two sidewalls and between the roof and floor was controlled within 97 mm and 75 mm, respectively, achieving a remarkable surrounding rock control effect. The findings can provide a reference for surrounding rock control in mining roadways under similar geological conditions.

Keywords

"Three-Soft" Coal Seam; Mining Roadway; Full-Section Anchor Cable; Floor Grouting Anchor Cable

1. Introduction

In recent years, with the advancement of support theories and the improvement of support technologies for mining roadways [1–5], the support challenges associated with mining roadways under "three-soft" coal seam conditions have been

progressively resolved. However, due to variations in seam occurrence conditions, investigating rational support methods tailored to specific geological settings remains of practical significance for the extraction of "three-soft" coal seams [6–10]. The main coal seam mined at Xingcun Coal Mine is the II₁ seam, which exhibits considerable thickness variation. The mining roadways are driven along the floor, with the roof coal thickness varying unevenly, generally around 1.0 m or even greater in some sections. The seam occurrence is characterized by typical "three-soft" coal seam features developed under the influence of sliding tectonic structures.

For an extended period, the excavation and support of the mine's roadways have been extremely challenging. When supported by U-shaped steel arches, the maintenance length of the coal roadway has not exceeded 200 m, and repeated repairs have been required, severely hindering the rapid advancement of the working face and the high-yield, high-efficiency production of the mine.

In response to the production geological conditions of the II₁ coal seam at Xingcun Coal Mine, the mine has been continuously exploring rational support forms for its mining roadways. Based on borehole inspection of surrounding rock fractures and through numerical simulation, this study determines a rational support scheme for the mining roadway—namely, a full-section support approach combining "U-shaped steel arch + full-section anchor cables + surrounding rock grouting"—and establishes appropriate support parameters. This ensures roadway stability during excavation and lays the foundation for safe and efficient mining at the working face.

2. Mine Production Geological Conditions

The 12011 working face is located in the eastern wing of the No. 12 mining district of Xingcun Coal Mine, with the 12031 goaf to the north, unmined areas to the south, the eastern wing return-air downhill roadway to the west, and the mine boundary to the east. The mining engineering plan is shown in Fig. 1. The main coal seam mined is the II₁ seam, which is extremely soft and fragmented—it crumbles into powder upon hand kneading—with a Protodyakonov coefficient (f) of 0.2–0.3. Within the 12011 working face, the coal seam strike ranges from 70° to 85°, the dip direction from 340° to 355°, and the dip angle from 14° to 19°, averaging 15°. The burial depth varies from 267 m to 243 m. The coal thickness ranges from a maximum of 7 m to a minimum of 1.8 m, with an average thickness of 4.37 m. The coal seam exhibits a simple structure, with localized partings ranging from 0.1 m to 0.4 m in thickness. Influenced by sliding tectonic structures, the roof and floor of the coal seam undulate by 0.3 m to 1.7 m along both the strike and dip directions, displaying a "chicken-nest" morphology characterized by abrupt thickening and thinning over short distances. This results in a loose fabric, low strength, predominantly powdery coal with occasional blocky intercalations, and a high susceptibility to caving and rib spalling.

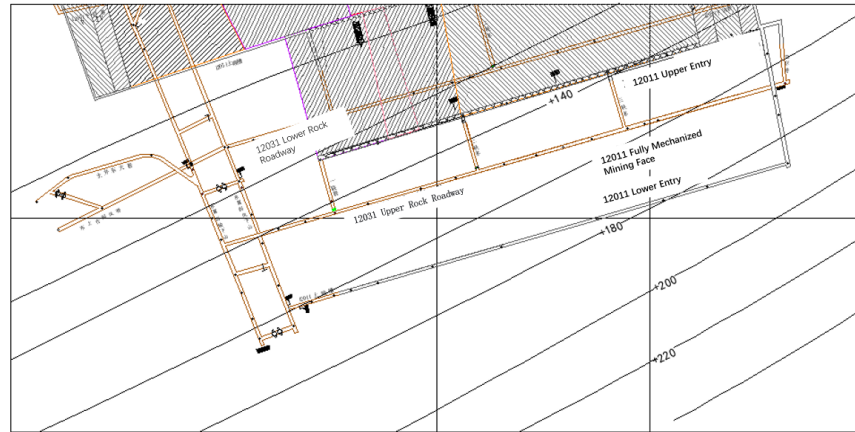


Figure 1. Plan of excavation works

According to borehole statistics from the mining area and its surroundings, combined with actual exposure and mining analysis of the adjacent 12031 fully mechanized working face, the roof of the II₁ coal seam consists primarily of mudstone, followed by sandy mudstone, fine- to medium-grained sandstone, and locally, siltstone. The floor is mainly composed of mudstone, with sandy mudstone as the secondary lithology. Borehole wall observation was employed to investigate the distribution and structure of the roof strata. Within a range of 13.0–17.0 m above the coal seam roof, the strata consist of argillaceous sandstone and carbonaceous mudstone, exhibiting a muddy texture and cementation, and are prone to swelling upon contact with water. Borehole probing was used to test the strength of the coal and rock mass within a 10 m zone above the roof and a corresponding 10 m zone into the coal sidewalls. The results indicate an average strength of 26.54 MPa for the argillaceous sandstone in the roof and 19.57 MPa for the carbonaceous mudstone.

3. Field Test of Fracture Development in Surrounding Rock of 12011 Upper Entry

3.1. Monitoring Station Layout

To understand the fracture propagation law of the surrounding rock in the upper entry of the 12011 working face, and to provide a basis for determining grouting parameters and anchor cable length, a total of 12 peep holes were arranged in the roof, with a designed hole depth of 10 m, as shown in Table 1.

Table 1: Viewing Hole Distribution Statistics

Roadway	Diameter (m)	Hole Numbe	Hole Location (Facing Direction)	Actual Viewing Hole Diameter (m)	Remarks
12011 Work Surface Top Shutter Plate	20	1#	Center of plate	9.78	
	40	2#	Left side	10.0	
		3#	Center of plate	9.92	
		4#	Right side	9.92	
	60	5#	Center of plate	9.6	

	80	6#	Left side	9.95	
		7#	Center of plate	9.18	
		8#	Right side	9.75	
	100	9#	Center of plate	9.9	
	130	10#	Left side	9.84	
		11#	Center of plate	9.92	
12#		Right side	9.93		
12011 Work Surface Top Shutter Plate	80	1#	Right side bottom plate 1.3m	5.75	Inclination 15°
		2#	Left side bottom plate 1m	5.65	Inclination 12°
	40	3#	Right side bottom plate 1.2m	4.48	Inclination 27°
		4#	Left side bottom plate 1m	5.75	Inclination 11°

3.2. Peep Results and Analysis

Based on the analysis of surrounding rock borehole imaging data, and a comprehensive evaluation of surrounding rock hardness, integrity, and the development degree of fractures in each borehole, Figure 2 presents a summary diagram of the roof borehole imaging at measuring points from 20 m to 130 m of the 12011 upper entry.

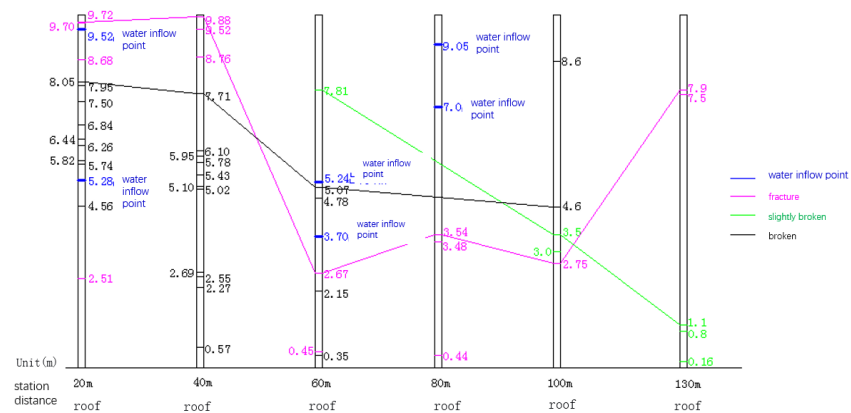


Figure 2. Schematic cross-sectional diagram of the failure range of observation boreholes (direct roof) at chainages from 20 m to 130 m in the 12011 upper entry

As shown in Fig. 2, the surrounding rock damage observed in the roof boreholes between chainage 20 m and 60 m is relatively extensive, with fractured and broken zones extending to the deepest part at the borehole bottom. Water seepage through fractures was observed at depths of 5.28 m and 9.52 m in the roof borehole at chainage 20 m, at 3.7 m and 5.24 m in the roof borehole at chainage 60 m, and at 7.0 m and 9.05 m in the roof borehole at chainage 80 m. In contrast, the surrounding rock damage in the roof boreholes between chainage 80 m and 130 m is comparatively mild. The roof damage is relatively minor near the heading face, with deformation becoming progressively more severe toward the rear of the roadway.

The borehole inspection results reveal the following:

- ① The surrounding rock of the roadway as a whole exhibits a trend of increasing damage with the time elapsed after excavation. This trend has not been effectively controlled, and in early-stage roadways, the damage has already reached the critical position corresponding to the anchorage length, with the potential for further propagation into deeper zones.
- ② No water outflow was observed during roadway excavation; however, distinct water seepage points were detected in multiple boreholes during this inspection. This indicates that the dynamic pressure induced by roadway driving has exerted a certain influence on the surrounding water pressure, causing changes in water flow pathways and resulting in water seepage within the roof strata of the already driven roadway. This phenomenon adversely affects both the support structure and the surrounding rock, posing a significant threat to the stability of the formed roadway. Corresponding countermeasures should therefore be incorporated into the support design.
- ③ The fracture distribution range in the roof provides a basis for determining the appropriate anchor cable length.
- ④ During sidewall borehole drilling with the anchor cable drilling rig, poor slag discharge resulted in a considerable amount of coal fines remaining in the boreholes, making it difficult to obtain a clear view of the full borehole profile. Nevertheless, the inspection results from the No. 1–4 sidewall boreholes in the upper cross-heading of the 12011 working face indicate that the sidewall boreholes achieved favorable hole-forming quality and are suitable for anchor cable installation.

4. Surrounding Rock Control Technology for Mining Roadways in "Three Soft" Unstable Coal Seams

4.1. Connotation of Full-Section Synergistic Support

In response to the coal seam occurrence conditions at Xingcun Coal Mine, this study proposes a combined active–passive synergistic support approach, employing U-shaped steel arches as high-strength surface-retaining components and full-section anchor cables with grouting as the primary control method.

The coal seam thickness is unstable in its occurrence. Under certain conditions, the roof consists of a coal layer less than 1.0 m thick; in individual cases, the top coal is even thicker. Previous practice has demonstrated that rock bolt support offers limited effectiveness, with unreliable anchoring force and even roof collapse and fallouts occurring in some instances. Rock bolts fail to provide timely support and high pre-tensioning force, and conventional surface-retaining components such as W-shaped steel straps and rebar ladder beams provide relatively low working resistance to the roadway surrounding rock. Therefore, this study proposes the adoption of U-shaped steel arches as high-strength surface-retaining components.

Active support represented by rock bolts, anchor cables, and grouting has become the primary approach for roadway surrounding rock control. Based on the occurrence conditions of the "three-soft" unstable coal seam, this study proposes full-section anchor cables and grouting as the main control methods. First, taking advantage of the deep anchorage characteristics of anchor cables, the internal anchorage end is placed within the relatively stable deep rock mass, thereby mobilizing the bearing capacity of the deep stable strata. Second, floor anchor cables exert a substantial anchoring force on the floor, integrating the roadway surrounding rock into a unified bearing structure and effectively controlling floor heave. Third, grouting enhances the integrity of the soft surrounding rock and increases its deformation resistance capacity.

4.2. Numerical Simulation Analysis of Surrounding Rock Control by Full-Section Synergistic Support

Based on the foregoing analysis, a combined active–passive synergistic support approach is proposed, employing U-shaped steel arches as high-strength surface-retaining components and full-section anchor cables with grouting as the primary control method. To analyze the effectiveness of this synergistic support approach, four support schemes were preliminarily defined for comparative analysis. The support parameters for each scheme are as follows:

Scheme I: U-shaped steel arch support. Grade 36U steel sections are used, with an arch spacing of 700 mm.

Scheme II: U-shaped steel arch support + roof and sidewall anchor cables. The U-shaped steel arches use Grade 36U sections, with an arch spacing of 700 mm. The anchor cables are $\Phi 22$ mm \times L8300 mm, with a sidewall anchor cable row spacing of 600 mm \times 700 mm and a roof anchor cable row spacing of 1000 mm \times 700 mm. A pre-tensioning force of 150 kN is applied to the anchor cables.

Scheme III: U-shaped steel arch support + full-section anchor cables. Building upon Scheme II, three additional anchor cables of $\Phi 22$ mm \times L8300 mm are installed in the floor, with a sidewall anchor cable row spacing of 600 mm \times 700 mm, a roof anchor cable row spacing of 1000 mm \times 700 mm, and a floor anchor cable row spacing of 1700 mm \times 2000 mm. A pre-tensioning force of 150 kN is applied to the anchor cables.

Scheme IV: U-shaped steel arch support + full-section anchor cables + grouting. Building upon Scheme III, full-section grouting reinforcement is implemented.

1. Model Construction and Calculation Parameters

FLAC3D was adopted for the numerical simulation study. Based on the geological conditions of the II₁ coal seam mining engineering at Xingcun Coal Mine, the following assumptions were made when conducting the simulation with FLAC3D:

(1) The influence of temperature and gas pressure fields on the simulation results is not considered, and the spatial positions around the model remain unchanged.

(2) Each coal and rock stratum in the model is treated as an elastoplastic, homogeneous, and continuous rock mass.

(3) All five boundaries except the top surface are fixed boundaries. The weight of the overlying strata is considered, with a load of 5.75 MPa applied at the top and a horizontal stress of 6.6 MPa.

(4) The roadway excavation process and the effects of mining-induced stresses exert no influence on the final stress distribution characteristics of the surrounding rock.

(5) Mesh discretization is relatively dense in the vicinity of the studied roadway and in stress concentration zones.

(6) The influence of stresses around the roadway is treated as a plane strain problem.

To more closely approximate actual engineering conditions, the FLAC3D numerical calculation software was employed for this simulation, with the large-strain mode adopted to establish the computational model and conduct refined numerical simulation. The model measures 65 m in length, 55 m in height, and 2 m in the excavation direction, with an average strata dip angle of 15°. The mining roadway was preliminarily designed with a straight-wall curved-arch cross-section, with section dimensions of 4.2 m × 3.5 m and a straight wall height of 1.8 m. During the calculation process, horizontal displacement was constrained on the lateral boundaries of the model, and vertical displacement was constrained on the bottom boundary. The model comprises a total of 58,460 elements and 77,928 nodes. Based on the roof and floor strata distribution of the II₁ coal seam (see Table 2), the established numerical calculation model is shown in Fig. 3.

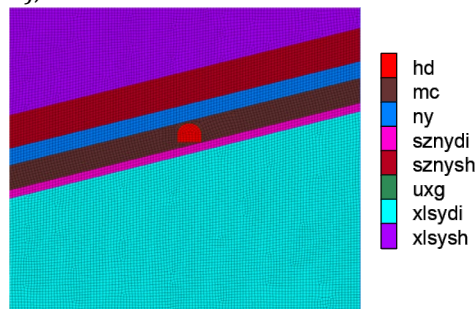


Figure 3. Numerical calculation model

(hd—roadway; mc—coal seam; ny—mudstone; sznydi—floor sandy mudstone; sznysh—roof sandy mudstone; uxg—U-shaped steel; xlsydi—floor fine-grained sandstone; xlsysh—roof fine-grained sandstone)

Table 2. Layer 2 Coal Seam Roof Rock Lithology Table

Name	Rock Type	Thickness (m)
Roof Plate	Medium-coarse grained sandstone (major component)	20
	Silty mudstone	6.0

	Mudstone	3.0
Coal Seam	Layer 2-1 Coal	4.5
Floor Plate	Silty mudstone	1.5
	Fine-grained sandstone	20

The Mohr-Coulomb yield criterion is adopted to determine the failure of rock masses.

$$f_s = \sigma_1 - \sigma_3 \frac{1 + \sin \varphi}{1 - \sin \varphi} - 2c \sqrt{\frac{1 + \sin \varphi}{1 - \sin \varphi}} \quad (1)$$

In Equation (1), σ_1 and σ_3 are the maximum and minimum principal stresses, respectively, and c and φ are the cohesion and friction angle, respectively. When $f_s > 0$, shear failure of the material occurs. Under normal stress conditions, the tensile strength of rock masses is very low; therefore, whether tensile failure occurs in the rock mass can be determined according to the tensile strength criterion ($\sigma_3 \geq \sigma_t$).

Based on the field geological investigation and the rock mechanics test results provided by related studies, considering the scale effect of rock, the strain-softening characteristics after rock mass failure are adopted. The rock mass mechanical parameters are selected accordingly. The rock mass mechanical parameters used in the numerical simulation are presented in Table 3.

Table 3. Rock Mechanical Parameters for Numerical Simulation

Rock Type	Density (kg/m ³)	Elastic Modulus (GPa)	Shear Modulus (GPa)	Bulk Modulus (MPa)	Internal Friction Angle (°)
Fine-grained sandstone	2500	2.5	2.23	3.7	26
Silty mudstone	2500	2.53	2.14	3	25
Mudstone	2500	2.42	2.16	2.9	25
Coal	1480	1.23	1.08	1	21

2. Simulation Process

Based on the geological conditions and the objectives of the calculation, the numerical simulation process primarily includes the following steps:

(1) A computational model is established based on the physical prototype of the in-situ mining conditions. The boundary mechanical and displacement conditions are prescribed or constrained, and equilibrium of the initial stress field (prior to excavation disturbance) is achieved to ensure the validity of the calculation results.

(2) The roadway is excavated, and the deformation characteristics, failure process, and evolution patterns of the surrounding rock under unsupported conditions (bare roadway) are analyzed, providing a baseline for subsequent comparative analysis with the calculation results of the support schemes.

(3) The stress field, plastic zone distribution, and displacement distribution characteristics of the roadway surrounding rock under the four support schemes

are calculated and comparatively analyzed.

3. Simulation Results and Analysis

(1) Distribution of the Plastic Zone in the Roadway Surrounding Rock

Figs. 4 to 8 present the plastic zone distribution in the roadway surrounding rock under the unsupported condition and the four support schemes. As can be observed from the figures, the failure mode of the roadway surrounding rock is predominantly shear failure, with tensile failure occurring in the roadway floor. The plastic zone is oriented consistently with the dip angle of the coal and rock strata. Under the unsupported condition, the plastic zone in the roadway surrounding rock is relatively extensive: the maximum extent reaches approximately 16 m from the roadway sidewall, the roof plastic zone extends approximately 3.4 m from the roadway surface, and the floor plastic zone extends approximately 2 m from the roadway surface, indicating a large fractured zone in the roadway surrounding rock. Under the U-shaped steel arch support condition, the plastic zone in the roadway surrounding rock exhibits a modest reduction in extent. Under the U-shaped steel arch + roof and sidewall anchor cable support condition, the plastic zone range is significantly reduced, with the maximum extent reaching approximately 14 m from the roadway sidewall. Under the U-shaped steel arch + full-section anchor cable support condition, the plastic zone is further diminished. Under the U-shaped steel arch + full-section anchor cable + grouting support condition, the grouting reinforcement integrates the roadway surrounding rock into a unified whole, and the constitutive model of the surrounding rock transitions from the Mohr–Coulomb model to a strain-softening model, resulting in an increase in the extent of the plastic zone.

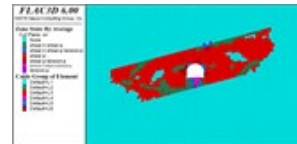


Figure 4. Distribution of plastic zone in surrounding rock under unsupported condition

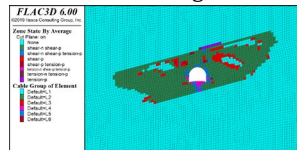


Figure 5. Distribution of plastic zone in surrounding rock under U-shaped steel support

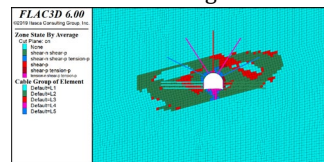


Figure 6. Distribution of plastic zone in surrounding rock under U-shaped steel + roof and rib anchor cable support

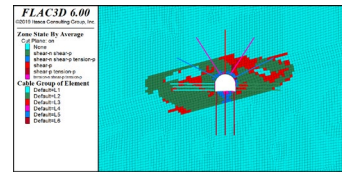


Figure 7. Distribution of plastic zone in surrounding rock under U-shaped steel + full-section anchor cable support

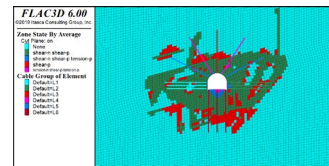


Figure 8. Distribution of plastic zone in surrounding rock under U-shaped steel + full-section anchor cable + grouting support

(2) Analysis of Horizontal Displacement of the Roadway Surrounding Rock

Under the unsupported condition, the deformation of the left sidewall reached 227 mm, and that of the right sidewall reached 207 mm, indicating substantial horizontal deformation of the roadway surrounding rock. Under the U-shaped steel arch support condition, the horizontal displacement of the surrounding rock decreased, with the displacements of the left and right sidewalls reduced to 197 mm and 185 mm, respectively. A tendency for horizontal displacement to transfer toward the floor corners was observed, exerting a certain influence on the stability of the roadway floor. Under the U-shaped steel arch + roof and sidewall anchor cable support condition, the deformation of the left sidewall was 110 mm and that of the right sidewall was 109 mm. The roof and sidewall anchor cables contributed to a reduction in sidewall displacement; however, pronounced displacement concentration phenomena emerged at the roof corners and floor corners of the roadway. Under the U-shaped steel arch + full-section anchor cable support condition, the deformation of the left sidewall was further reduced to 107 mm and that of the right sidewall to 102 mm, indicating a continued reduction in roadway deformation. Under the U-shaped steel arch + full-section anchor cable + grouting support condition, the deformation of the left sidewall was 98 mm and that of the right sidewall was 99 mm. While the horizontal displacement of the surrounding rock was similar to that under the U-shaped steel arch + full-section anchor cable support condition, the displacement concentration at the roof and floor corners was alleviated. The displacement was more uniformly distributed across the two sidewalls, thereby avoiding displacement concentration at the roof and floor corners and proving more conducive to the long-term stability of the roadway support. A comparison of the horizontal displacements under the different support schemes is presented in Fig. 9.

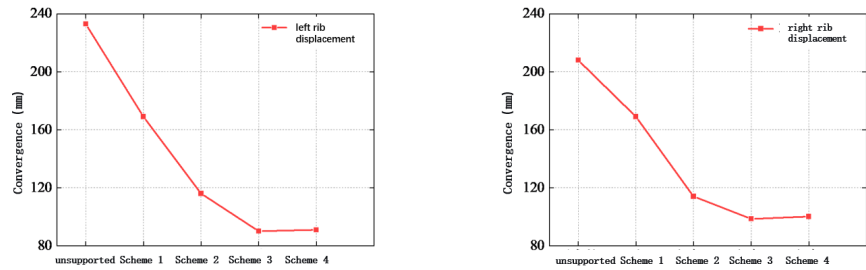


Figure 9. Comparison of roadway horizontal displacement under different support schemes

(3) Analysis of Vertical Displacement of the Roadway Surrounding Rock

Under the unsupported condition, the roof displacement of the roadway reached 236 mm and the floor heave was 196 mm, indicating substantial vertical deformation of the roadway surrounding rock. Under the U-shaped steel arch support condition, the roof displacement was reduced to 185 mm; however, the floor heave increased to 277 mm. This indicates that while the roof deformation was alleviated under the U-shaped steel arch support, the displacement was transferred to the roadway floor, exerting a certain adverse effect on floor support. Under the U-shaped steel arch + roof and sidewall anchor cable support condition, the roof deformation was 98 mm and the floor heave was 180 mm. Compared with the U-shaped steel arch support alone, both the roof and floor displacements were reduced to varying degrees. Under the U-shaped steel arch + full-section anchor cable support condition, the vertical displacement of the surrounding rock was further reduced, with a roof deformation of 96 mm and a floor heave of 159 mm. Under the U-shaped steel arch + full-section anchor cable + grouting support condition, the roof deformation was 90 mm and the floor heave was 150 mm. This scheme yielded the smallest vertical deformation of the roadway surrounding rock and was most conducive to the long-term stability of the roadway support. A comparison of the roof and floor displacements under the different support schemes is presented in Fig. 10.

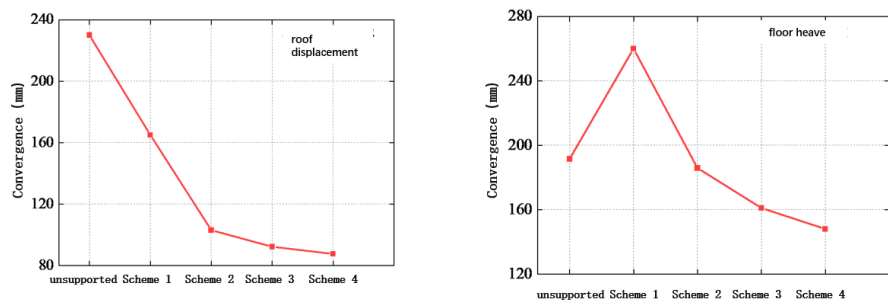


Figure 10. Comparison of roof-to-floor displacement under different support schemes

5. Engineering Applications

5.1. Support Plan and Parameters

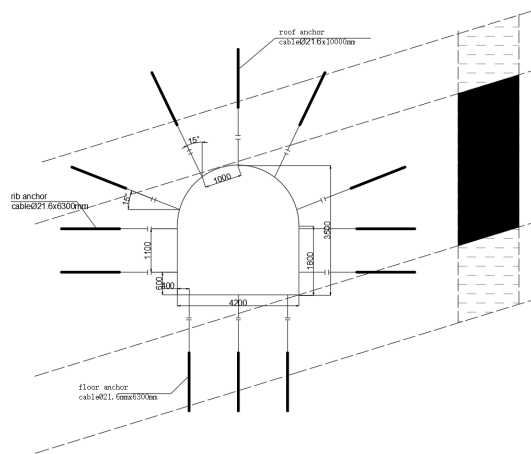


Figure.11 Roadway full section anchor cable layout section diagram

Roof and sidewall anchor cables: The anchor cables have a diameter of 21.6 mm and are available in two lengths: 10.0 m and 6.3 m. The borehole diameter is 28 mm. For anchorage, one K2350 resin cartridge and three Z2350 resin cartridges are used, achieving an anchorage length of no less than 2 m. The anchor cables are installed perpendicular to the rock face. The pre-tensioning force applied to the anchor cables is not less than 200 kN. Each anchor cable is fitted with a 300 × 300 × 14 mm arched steel bearing plate, with an arch height of no less than 60 mm. U-shaped steel arches combined with metal mesh and plastic mesh are used for surface retention.

Floor anchor cables: High-strength prestressed birdcage anchor cables with specifications of $\phi 21.6 \times 6300$ mm are employed. The cable beam base plate is made of 14# channel steel with a length of 2400 mm. The pre-tensioning force applied to the anchor cables is not less than 200 kN, and the cable row spacing is 2000 mm. Grouted anchorage is adopted, with a borehole diameter of 60 mm and Grade 42.5 cement as the grouting material.

Surrounding rock grouting: A combined shallow- and deep-hole grouting method is adopted. The shallow holes have a length of 2000 mm, while the deep-hole lengths are as follows: grouting holes at the floor and sidewall bottom corners are 4000 mm deep, and all other grouting holes are 5000 mm deep. Special grouting hole sealers are used for hole sealing, with the sealing depth adjustable between 500 mm and 1000 mm. The grouting hole row spacing is 1400 mm, with a hole spacing of 1400 mm for roof holes and 800 mm for sidewall holes. Ordinary cement grout is used as the grouting material, with P.O 42.5 ordinary Portland cement. The water–cement ratio of the grouting slurry is water : cement = 1 : 0.6–0.8, and the grouting pressure does not exceed 2.0 MPa.

5.2. Support Effectiveness

To evaluate the effectiveness of the synergetic support scheme of "U-shaped steel arch + full-section anchor cables + grouting," observation points were arranged to monitor the deformation of the roadway surrounding rock. Fig. 12 presents the variation curves of the roof and sidewall convergence in the upper cross-heading of the 12011 working face.

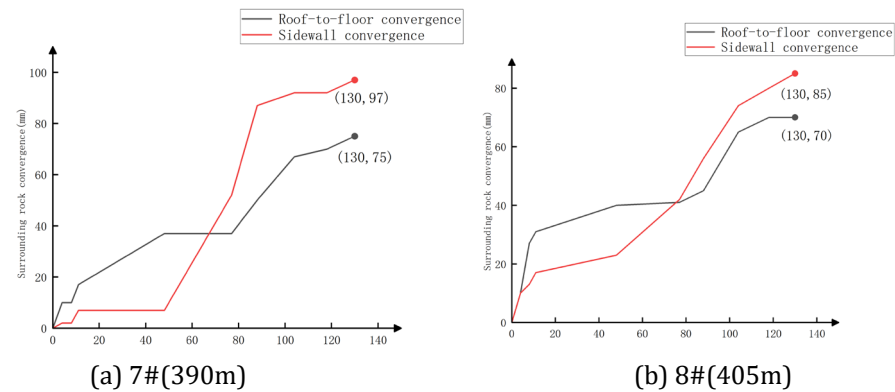


Figure 8. The amount of movement of roof and two groups at "U-type steel bracket + full-section anchor cable + grouting" synergistic support zone

The monitoring results indicate the following:

- ① Within the observation interval, the maximum roof-to-floor convergence recorded at the two monitoring stations was 75 mm, which did not affect waste rock transport during roadway excavation and did not necessitate floor dinting.
- ② During the observation period, the maximum sidewall deformation of the roadway was 97 mm, and the cumulative roof-to-floor convergence was 75 mm. The U-shaped steel arches exhibited no significant structural deformation, and the passive support strength of the U-shaped arches gradually increased over time.
- ③ In the early stage of roadway excavation, the roof-to-floor deformation exceeded that of the sidewalls. As time progressed, the sidewall deformation increased gradually, whereas the roof-to-floor deformation increased slowly, with the sidewall deformation eventually exceeding the roof-to-floor deformation. This also indicates that the addition of floor grouted anchor cables and grouting effectively controlled floor heave.

6. Conclusions

(1) Borehole inspection was employed to investigate the fracture development in the surrounding rock of the "U-shaped steel arch + roof and sidewall anchor cable" supported section of the 12011 working face return-air roadway. The results show that the roadway surrounding rock as a whole exhibits a trend of progressively worsening damage with increasing time elapsed after excavation, and this trend has not been effectively controlled. No distinct roadway excavation stabilization zone was observed in terms of deformation. Within 30 m from the heading face, the maximum fracture depth in the roadway roof ranges from 7.5 m to 7.9 m, and the

deformation becomes increasingly severe toward the rear of the roadway. Beyond 90 m from the heading face, the roof boreholes reveal a relatively extensive zone of surrounding rock damage, with the roof failure depth exceeding 10 m. The failure depth of the roadway sidewalls exhibits a zonal failure pattern, being relatively fragmented within 2.0 m and again between 4.5 m and 5.0 m.

(2) In response to the coal seam occurrence conditions at Xingcun Coal Mine, numerical simulation was conducted to analyze the surrounding rock control effectiveness under different support schemes. The plastic zone distribution and displacement characteristics of the roadway surrounding rock were compared and analyzed under four support schemes: U-shaped steel arch support alone; U-shaped steel arch + roof and sidewall anchor cables; U-shaped steel arch + full-section anchor cables; and U-shaped steel arch + full-section anchor cables + grouting. The differences among these schemes in controlling surrounding rock stability were elucidated, providing a reference for determining roadway support parameters. On this basis, a combined active-passive full-section synergistic support approach was proposed, employing U-shaped steel arches as high-strength surface-retaining components and full-section anchor cables with grouting as the primary control method, and the connotation of full-section synergistic support was expounded.

(3) With the adoption of the "U-shaped steel arch + full-section anchor cables + grouting" support scheme, the deformation of the roadway surrounding rock and the floor heave were significantly reduced. The surrounding rock deformation remained within a controllable range, the roadway profile was well maintained, and normal operation of the roadway was not affected. These results indicate that the proposed roadway control technology and parameter design are reasonable, laying a foundation for the safe and efficient mining of "three-soft" unstable coal seams.

References

- [1] Kang, H. P. (2021). Seventy years of development and prospects of surrounding rock control technology for coal mine roadways in China. *Chinese Journal of Rock Mechanics and Engineering*, 40(1), 1-30.
- [2] Hou, C. J. (2013). *Surrounding rock control in roadways* (pp. 288-390). Xuzhou: China University of Mining and Technology Press.
- [3] Li, G. C., Yang, S., Sun, Y. T., et al. (2022). Research progress on surrounding rock control technology for roadways under complex conditions. *Coal Science and Technology*, 50(6), 29-45.
- [4] Zhang, P. (2023). Supporting technology for high-stress "three-soft" coal seam roadway under sliding structure. *Coal Science & Technology Magazine*, 44(2), 151-156.
- [5] Su, J. H., Ren, J. W., Xin, Y. J., et al. (2023). Support technology for mining roadways with fractured roof in close-distance sliding structure zones. *Energy and Environmental Protection*, 45(8), 277-283.
- [6] Wang, X. K., Xie, W. B., Jing, S. G., et al. (2018). Experimental study on large deformation control mechanism of extremely loose coal roadway surrounding rock in sliding structure zones. *Chinese Journal of Rock Mechanics and Engineering*, 37(2), 312-324.
- [7] Liu, C. X. (2006). Analysis of the characteristics of the Huadong sliding structure in Songshan, Henan. *Zhongzhou Coal*, 143, 24-25.

- [8] Song, C. S., Zhu, Q. Q., Ren, J. W., et al. (2022). Study on in-situ stress characteristics of coal mines in sliding structure zones. *Coal Technology*, 41(9), 1–5.
- [9] Qin, J. B. (2016). Application study on synergistic support of U-shaped steel arch combined with anchor cables and cable grouting. *Coal Mine Modernization*, 4, 38–40.
- [10] He, S. P., Li, F. L., Gou, P. F., et al. (2025). Reform and practice of mining roadway support in "three-soft" coal seams at Xingcun Coal Mine. *Energy and Environmental Protection*, 47(4), 274–281.